Decay studies of ^{170,171}Au, $^{171-173}$Hg, and ^{176}Tl

H. Kettunen, T. Enqvist, T. Grahn, P. T. Greenlees, P. Jones, R. Julin, S. Juutinen, A. Keenan, P. Kuusiniemi, M. Leino, A.-P. Leppänen, P. Nieminen, J. Pakarinen, P. Rahkila, and J. Uusitalo
Department of Physics, University of Jyväskylä, P.O. Box 35, FIN-40014 Jyväskylä, Finland
(Received 9 December 2003; published 28 May 2004)

The ^{170,171}Au isotopes were produced in the fusion-evaporation reaction of a ^{78}Kr ion beam with a ^{96}Ru target. For ^{170}Au the proton and α emission from the ground state were observed for the first time and the decay of the isomeric state was measured with improved accuracy. In addition, the decay of ^{171}Au was measured with high statistics. A new α-emitting nucleus ^{171}Hg and the previously known ^{172}Hg and ^{167,168,169,170}Pt isotopes were also studied. The ground-state proton emission was identified for a new proton emitter ^{176}Tl using the fusion-evaporation reaction of ^{78}Kr ions with a ^{102}Pd target. The previously known proton emitter ^{177}Tl and α-decaying nucleus ^{173}Hg were also identified in this reaction. The fusion products were separated in-flight using a gas-filled recoil separator and implanted into a position-sensitive silicon detector. Identification of the nuclei was based on position, time, and energy correlations between the implants and subsequent decays.

DOI: 10.1103/PhysRevC.69.054323 PACS number(s): 23.50.+z, 23.60.+e, 27.70.+q, 21.10.Dr

I. INTRODUCTION

Proton radioactivity provides a unique possibility to probe nuclear structure far from stability. The measured proton separation energies test the validity of different mass formulae on the edge of the nuclear landscape beyond the proton drip line. The proton emission probability is extremely sensitive to the energy and to the angular momentum of the emitted proton. This offers possibility to deduce the structure of the state involved in the proton emission by comparing the experimental proton half-life to theoretically predicted values. The known proton emitting nuclei above the $N=82$ neutron shell closure are predicted to be nearly spherical [1]. The decay properties of these spherical proton emitters are well described by various theoretical models [2,3]. In deformed nuclei, below the closed $N=82$ neutron shell, proton emission can be used to estimate the degree of nuclear deformation, see Refs. [4–6], and references therein.

The orbitals available for the proton emission in neutron-deficient nuclei in the $64<Z<82$ region are the nearly degenerate $s_{1/2}$, $d_{3/2}$, and $h_{11/2}$ orbitals [2,7]. For odd-Z even-N proton emitting nuclei, above the $N=82$ shell closure, the ground-state proton emission is deduced to originate from the $\pi s_{1/2}$ orbital [2,8,9]. Correspondingly, the isomeric proton emission of these nuclei is deduced to originate from the $\pi h_{11/2}$ orbital.

Unlike in odd-even nuclei, in odd-odd proton emitters, above $N=82$ and for $64<Z<82$, the ground-state proton emission is deduced to originate from the $\pi d_{3/2}$ orbital [2,10–12], but the isomeric proton emission is deduced to originate from the $\pi h_{11/2}$ orbital similarly to the odd-even nuclei. The emergence of the $\pi d_{3/2}$ orbital below the $\pi s_{1/2}$ orbital in odd-odd proton emitters was explained by the coupling of the $\pi d_{3/2}$ proton with the $\nu f_{7/2}$ neutron [2]. According to Nordheim's strong rule [13,14] the state which has the lowest spin of the multiplet is dropped well below the other states in this configuration.

In the present work, the ground-state proton emission of the odd-odd nuclei ^{170}Au$_{91}$ and ^{176}Tl$_{95}$ has been identified for the first time. In addition, the decay properties of a number of neutron-deficient platinum and mercury isotopes, including the new isotope ^{171}Hg, have been studied.

II. EXPERIMENT

In the present work, the ^{170}Au and ^{176}Tl isotopes were produced in the $p3n$-evaporation channel from the fusion reactions of ^{78}Kr ions with ^{96}Ru and ^{102}Pd targets, respectively. As a side product of the ^{170}Au measurement, a new mercury isotope ^{171}Hg was produced in the $4n$-evaporation channel. The ion beam was produced from enriched ^{78}Kr gas by the ECR ion source and was delivered to the target by the $K=130$ MeV cyclotron of the Accelerator Laboratory at the Department of Physics of the University of Jyväskylä (JYFL). The average beam intensities were approximately 5pnA and 8pnA in ^{170}Au and ^{176}Tl experiments, respectively, measured in a Faraday cup in front of the target. The total beam-on-target times were 90 h and 37 h, respectively.

Seven bombarding energies, varying from 361 MeV to 391 MeV in the middle of the ^{96}Ru target with a thickness of 500 μg/cm^2 and an enrichment of 96.52% were used in the ^{170}Au measurement. In the ^{176}Tl measurement three bombarding energies, varying from 380 MeV to 389 MeV in the middle of the enriched ^{102}Pd target with a thickness of 800 μg/cm^2 were used. Fine adjustment of the primary-beam energies of 380 MeV, 395 MeV, and 405 MeV of ^{78}Kr ions with charge states of 15^+, 16^+, and 16^+, respectively, was performed using a set of carbon foils in front of the target. Energy losses in the beam window, degrader foils, target, and also in the helium filling-gas of the separator were calculated using the SRIM2000 code [15].

Fusion-evaporation residues were separated in-flight from the primary-beam particles and other reaction products using the JYFL gas-filled recoil separator RITU [16]. The separated residues were focused and implanted into a position-sensitive silicon strip detector at the focal plane of the separator. Prior to implantation the residues passed through two

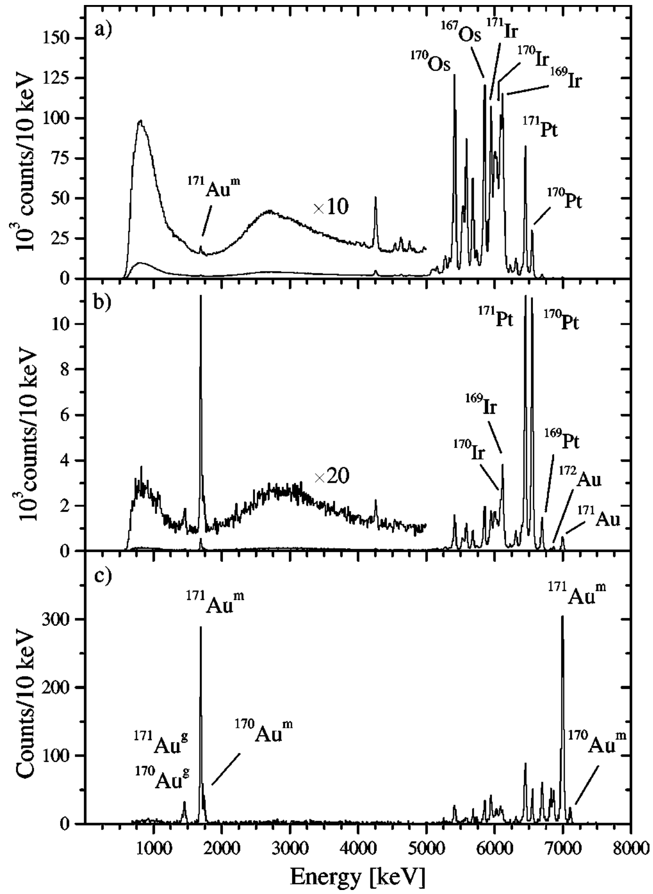

FIG. 1. (a) The energy spectrum observed in the silicon detector and vetoed with the gas counters and punch though detectors in the reaction ^{78}Kr+^{96}Ru. (b) The same data after requiring a position and time correlation with the implanted evaporation residues within a search time of 10 ms and (c) with an additional requirement of subsequent α decay in the same position within 200 ms search time and with decay energy between 6200 and 7200 keV.

multiwire proportional avalanche counters, placed 330 mm and 20 mm in front of the silicon detector, providing energy-loss and time-of-flight signals. The position-sensitive silicon detector of thickness 305 μm and of area 80×35 mm^2 was horizontally divided into 16, 5-mm wide position-sensitive strips. The vertical position resolution (full width) was better than 500 μm for implantations of fusion-evaporation residues and α decays and approximately 1000 μm for proton emissions in each strip. In the correlation procedure, the full width of the position window was approximately 1000 μm in the vertical direction. Two quadrant silicon detectors of area 60×60 mm^2 and thickness 450 μm were placed approximately 5 mm behind the position-sensitive silicon detector.

The energy-loss signals of the gas counters were used to separate the particle decays in the silicon strip detector from the implantations of scattered beam particles and evaporation residues. The gas counter placed 20 mm in front of the silicon detector was also used to detect the α particles emitted in the backward direction and only depositing part of their kinetic energy into the silicon detector before escaping from it. By vetoing the escaped α particles, the background in the region of typical proton emission energy, between 1 and 2.5 MeV is reduced considerably as can be seen in Fig. 1(a). The measured time-of-flight between the gas counters combined with the implantation energy in the silicon detector was used to separate the candidate fusion-evaporation products from scattered beam particles and transfer products. The quadrant silicon detectors behind the primary silicon detector were used to veto energetic protons and α particles which were able to punch through the position-sensitive silicon detector. The focal-plane detector system is described in more detail in Refs. [17,18].

TABLE I. Data used for α energy calibration.

Nucleus	E_α^{Ref} (keV)	Reference
^{167}Os	5853(5)	[23]
^{166}Os	6000(6)	[23]
^{170}Ir	6083(11)	[23]
^{169}Ir	6119(9)	[23]
^{168}Ir	6227(15)	[23]
^{172}Pt	6314(4)	[30]
^{171}Pt	6453(3)	[30]
^{170}Pt	6550(6)	[22]
^{169}Pt	6698(23)	[23]
^{172}Au	6860(10)	[34]
^{171}Au	6996(6)	[2]

The pressure of the helium filling-gas in RITU was 1.5 mbar. The gas volume of the separator was separated from the high vacuum of the cyclotron beam line by a 50 μg/cm^2 carbon foil. The common gas volume of the gas counters was filled with 3.0 mbar of isobutane and was isolated from the separator gas volume and the silicon detector high vacuum by 120 μg/cm^2 mylar foils. The silicon detectors were cooled to 253 K using circulating coolant.

The implanted evaporation residues were identified using the method of position and time correlation with the subsequent mother and daughter decays in the silicon detector [19,20]. For γ and x-ray detection at the focal plane, a Compton-suppressed Nordball-type germanium detector with 40% relative efficiency was placed adjacent to the silicon detector.

The α-decay energies measured in the silicon detector were calibrated using well-known α activities produced during the experiments. The α-active nuclei and the corresponding α energies E_α^{Ref} used for the calibration are shown in Table I.

The energies of the emitted protons are far away from the α-decay energies. In addition, the contribution of the pulse height defect and the energy of the recoiling daughter nucleus to the signal is different for protons and α particles in a silicon detector. Therefore, the final calibration of proton energies was performed using the previously measured proton energies of ^{171}Au and ^{177}Tl [2,9]. The data used for proton energy calibration are shown in Table II.

The energy resolution in the total α-particle energy spectrum sum of all 16 strips was measured to be 23 keV for the 6550(6) keV ^{170}Pt α peak. For proton emission the energy

TABLE II. Data used for proton energy calibration.

Nucleus	E_p^{Ref} (keV)	Reference
^{171}Au^{g}	1444(17)	[9]
^{171}Au^{m}	1692(6)	[2]
^{177}Tl^{m}	1958(10)	[9]

resolution was measured to be 20 keV for the 1692(6) keV ^{171}Au^{m} proton peak.

Since some of the activities measured in the present work are quite short lived, it is worth mentioning that the dead time of the data acquisition system used in the experiments was approximately 15 μs.

III. RESULTS AND DISCUSSION

A. Reaction ^{78}Kr + ^{96}Ru

The energy spectrum of all decay events from the ^{78}Kr + ^{96}Ru reaction observed in the silicon strip detector and vetoed with the gas counters and the punch through detectors is shown in Fig. 1(a). The spectrum is dominated by the activities produced in fusion-evaporation channels involving the evaporation of two or more charged particles. The effect of vetoing escaped α particles can be seen as a valley between 1 and 2.5 MeV. At the bottom of the valley a proton peak originating from the decay of ^{171}Au^{m} can be observed. The low-energy background extending down to 600 keV and cut by the electronic threshold is caused by β decays. Figure 1(b) shows the same data after requiring a position and time correlation with the preceding implantation of an evaporation residue within a search time of 10 ms. This selection suppresses effectively the longer-lived activities. Also the low-energy background is suppressed so that another proton decay peak can be observed. Figure 1(c) shows the data after the further requirement that the decay is followed by an α decay in the same position within a search time of 200 ms and with an α-decay energy between 6200 and 7200 keV. Decay peaks assigned to ^{170}Au and ^{171}Au in Fig. 1(c) were identified and separated using the decay properties of the subsequent daughter activities.

Two-dimensional mother and daughter decay energy plots of correlated decay chains of the type implantation–mother decay–daughter decay ($\mathrm{ER}-p_{\mathrm{m}}/\alpha_{\mathrm{m}}-\alpha_{\mathrm{d}}$) are shown in Figs. 2(a) and 2(b). Figure 2(a) shows the correlated decay chains where the proton emission of the mother nucleus is correlated with the α decay of the daughter nucleus. Figure 2(b) shows the correlated decay chains consisting of α decays. Maximum search times of 10 ms and 200 ms were used for mother and daughter decays, respectively.

As can be seen in Figs. 2(a) and 2(b), several mother decays are correlated strongly with two daughter activities which have clearly different α-decay energies. By studying the decay properties of the daughter activities it was observed that the daughters which have lower α-decay energies represent the α decays of the granddaughter activities. Since in the present work it is attempted to avoid correlations with

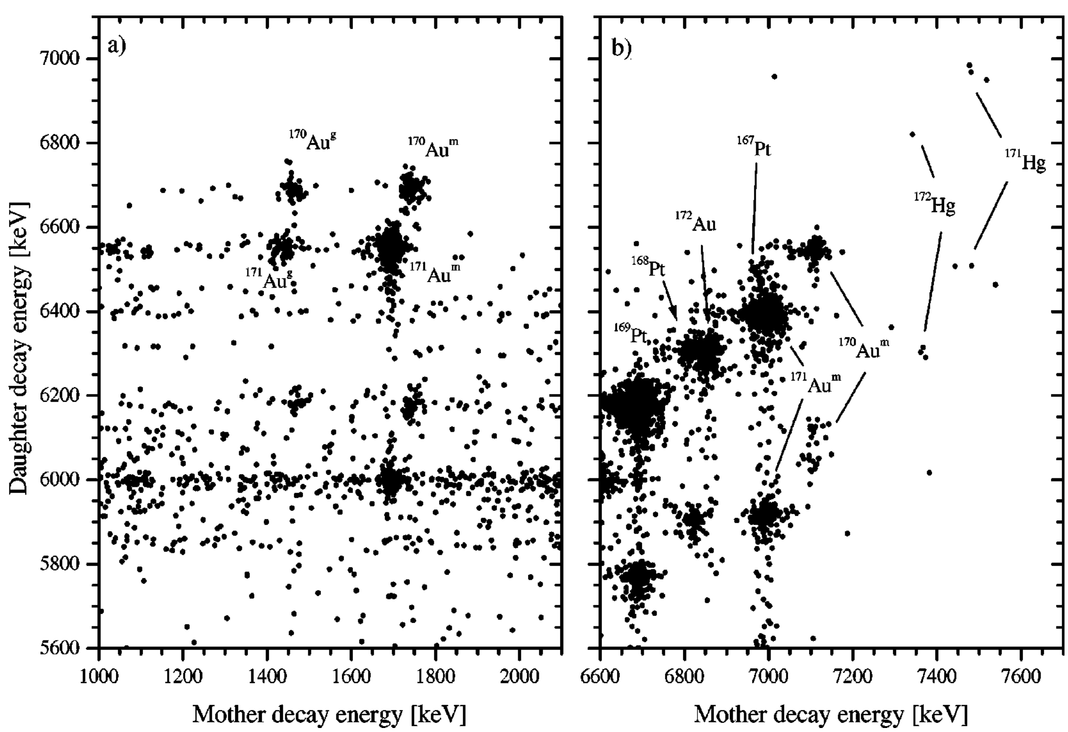

FIG. 2. Two-dimensional plot of the mother and daughter decay energies of correlated decay chains of the type $\mathrm{ER}-p_{\mathrm{m}}/\alpha_{\mathrm{m}}-\alpha_{\mathrm{d}}$ observed in the ^{78}Kr+^{96}Ru reaction. (a) Correlations where the proton decay of mother nucleus is followed by an α decay of the daughter nucleus ($\mathrm{ER}-p_{\mathrm{m}}-\alpha_{\mathrm{d}}$). (b) Correlated decay chains for α decays ($\mathrm{ER}-p_{\mathrm{m}}-\alpha_{\mathrm{d}}$). Maximum search times for the mother and daughter decays were 10 ms and 200 ms, respectively.

escaped α particles the mother decay can easily correlate directly with the α decay of the granddaughter nucleus. This happens if the α particle from the daughter decay escapes from the silicon detector and the half-lives of the nuclei in the decay chain are short compared to the search times used. In the present work the probability that an α particle deposits all its kinetic energy in the silicon detector is approximately 0.55. Correlations where the mother decay correlates directly with the granddaughter α decay can also be used as an additional confirmation in the identification of the mother nucleus. However, the final identification of the mother decay is based on the triple correlated ($\mathrm{ER}-d_{\mathrm{m}}-d_{\mathrm{d}}$) full-energy decay chains (d_{m} and d_{d} represent the mother and the daughter decays, respectively). In addition, quadruple correlated ($\mathrm{ER}-d_{\mathrm{m}}-d_{\mathrm{d}}-d_{\mathrm{gd}}$) full-energy decay chains were also searched for in some cases (d_{gd} corresponds to granddaughter decay).

B. The decay of ^{171}Au

1. The proton decay of ^{171}Au

Two previously known states decaying by proton emission in ^{171}Au [2,9,21] were observed in the present work. The identification of ^{171}Au was confirmed by $\mathrm{ER}-p_{\mathrm{m}}-\alpha_{\mathrm{d}}$ correlated decay chains as shown in Fig. 2(a).

The daughter activities of groups $^{171}\mathrm{Au}^{g}$ and $^{171}\mathrm{Au}^{m}$ in Fig. 2(a) were identified to originate from the α decay of the ground state in ^{170}Pt. The α-decay energy of $E_{\alpha}=6549(3)$ keV and half-life $T_{1/2}=14.3(6)$ ms were determined from 749 $\mathrm{ER}-p_{\mathrm{m}}-\alpha_{\mathrm{d}}$ correlated decay chains for the daughter activity of group $^{171}\mathrm{Au}^{m}$ in Fig. 2(a). Correspondingly, the α-decay energy of $E_{\alpha}=6548(4)$ keV and half-life $T_{1/2}=13(2)$ ms were obtained from 62 $\mathrm{ER}-p_{\mathrm{m}}-\alpha_{\mathrm{d}}$ correlated decay chains for the daughter activity of group $^{171}\mathrm{Au}^{g}$. The decay properties of the daughter activities in both groups are in good agreement with the α-decay properties of $E_{\alpha}=6550(6)$ keV and $T_{1/2}=14.7(5)$ ms reported for ^{170}Pt [22]. By combining the statistics of both groups an α-decay energy of $E_{\alpha}=6549(3)$ keV and half-life $T_{1/2}=14.2(6)$ ms were obtained for ^{170}Pt.

A large number of ^{170}Pt nuclei were also produced directly in the present experiment as can be seen in Figs. 1(a) and 1(b). An α-decay energy of $E_{\alpha}=6549(2)$ keV and half-life $T_{1/2}=14.0(2)$ ms were determined for the α-decay peak of ^{170}Pt in Fig. 1(b), being in good agreement with the previous values [22] (^{170}Pt α peak was used for the calibration, see Table I.) A search time of 500 ms was used for $\mathrm{ER}-\alpha_{\mathrm{m}}$ correlations and the half-life was determined by fitting to the exponential decay curve. It should be noted that part of the $\mathrm{ER}-\alpha_{\mathrm{m}}$ correlated decays of ^{170}Pt are not necessarily direct products of the fusion-evaporation reaction, since ^{170}Pt is the proton emission daughter nucleus of ^{171}Au. If the proton emitted in the decay of ^{171}Au escapes from the silicon detector, the decay of ^{170}Pt correlates directly with the implantation of the recoil. This would affect the half-life observed for ^{170}Pt. However, in the present case the effect of these events is negligible, since the number of ^{170}Pt α decays is approximately a hundred times larger than the number of protons emitted from ^{171}Au. In addition, the analysis for ^{170}Pt is based on the ^{170}Au part of the experiment where ^{171}Au nuclei were not produced in considerable quantities.

The isomeric state in ^{171}Au correlates directly also with the decay of the granddaughter nucleus with an α-decay energy of $E_{\alpha}=5998(3)$ keV. As an additional confirmation quadruple correlated full-energy decay chains were also searched for. From these decay chains a half-life of $T_{1/2}=200(20)$ ms was established for ^{166}Os. The obtained values are in good agreement with the previous results $E_{\alpha}=6000(6)$ keV and $T_{1/2}=220(7)$ ms [23] (The ^{166}Os α peak was used for the calibration, see Table I).

The previously measured proton energies of ^{171}Au and $^{177}\mathrm{Tl}^{m}$ [2,9] were used for the final proton energy calibration of the present work (see Table II). After the calibration a proton energy of $E_{\mathrm{p}}=1694(6)$ keV and half-life $T_{1/2}=1.13(5)$ ms were obtained for the proton emission from the $11/2^{-}$ isomeric state of ^{171}Au. Correspondingly, a proton energy of $E_{\mathrm{p}}=1437(12)$ keV and half-life $T_{1/2}=(22^{+3}_{-2})$ μs were established for the proton emission from the $1/2^{+}$ ground state. The decay properties are in good agreement with the previously measured results with $E_{\mathrm{p}}=1692(6)$ keV and $T_{1/2}=1.02(10)$ ms for the proton emission from the $11/2^{-}$ isomeric state [2] and $E_{\mathrm{p}}=1444(17)$ keV and $T_{1/2}=(17^{+9}_{-5})$ μs for the proton emission from the $1/2^{+}$ ground state of ^{171}Au [9]. In the recent in-beam γ-ray spectroscopic measurement of ^{171}Au [21] a somewhat shorter half-life of $T_{1/2}=1.014(9)$ ms was obtained for the decay of the $11/2^{-}$ isomeric state and for the decay of the $1/2^{+}$ ground state a longer half-life of $T_{1/2}=(37^{+7}_{-5})$ μs was given.

Figure 3(a) shows the $\mathrm{ER}-p_{\mathrm{m}}-\alpha_{\mathrm{d}}$ correlated proton energy spectrum for ^{171}Au where the α decay of ^{170}Pt is demanded as a daughter decay (α-decay energy between 6475 keV and 6610 keV). The time distributions of the decays in the proton peaks are shown in the inset panel. Figure 3(b) shows the corresponding spectra for the α decay of ^{171}Au. In the correlation the α decay of ^{167}Ir is demanded as a daughter decay (α-decay energy between 6345 keV and 6460 keV).

2. The α decay of ^{171}Au

The daughter activity of group $^{171}\mathrm{Au}^{m}$ in Fig. 2(b) was identified to originate from the α decay of the $11/2^{-}$ isomeric state in ^{167}Ir. An α-decay energy of $E_{\alpha}=6394(2)$ keV and half-life $T_{1/2}=25.7(8)$ ms were determined from 1151 $\mathrm{ER}-\alpha_{\mathrm{m}}-\alpha_{\mathrm{d}}$ correlated decay chains. The decay properties are broadly consistent with the previous results with $E_{\alpha}=6410(5)$ keV and $T_{1/2}=30.2(20)$ ms [2]. The α decay of ^{171}Au correlates strongly also with the decay of the granddaughter nucleus ^{163}Re with an α-decay energy of $E_{\alpha}=5917(3)$ keV. Using quadruple correlated full-energy decay chains a half-life of $T_{1/2}=260(40)$ ms was obtained for the granddaughter decay. The results are comparable with the previous values of $E_{\alpha}=5920(5)$ keV and $T_{1/2}=214(5)$ ms obtained for $^{163}\mathrm{Re}^{m}$ [2].

An α-decay energy of $E_{\alpha}=6995(4)$ keV and half-life $T_{1/2}=1.07(3)$ ms were obtained for the decay of $^{171}\mathrm{Au}^{m}$ using the $\mathrm{ER}-\alpha_{\mathrm{m}}-\alpha_{\mathrm{d}}$ correlated decay chains shown in Fig.

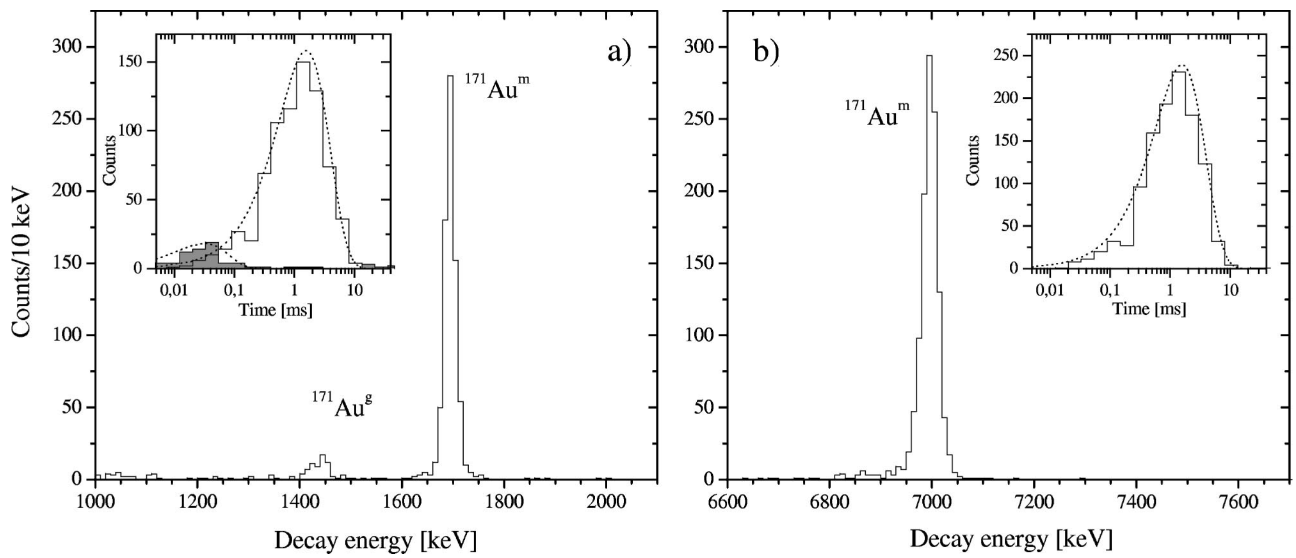

FIG. 3. Proton and α-particle energy spectra and time distributions for the decays of ^{171}Au. (a) The $(\mathrm{ER}-p_{\mathrm{m}}-\alpha_{\mathrm{d}})$ correlated proton energy spectrum for ^{171}Au where the α decay of ^{170}Pt is demanded as a daughter decay. Search times of 10 ms and 200 ms were used for mother and daughter decays, respectively. The time distributions of the ^{171}Au^{m} and ^{171}Au^{g} proton emissions in $\mathrm{ER}-p_{\mathrm{m}}-\alpha_{\mathrm{d}}$ correlated decay chains are shown as the solid line and the filled area, respectively, in the inset panel. For the time distributions a longer search time of 50 ms was used for the mother activity. The dotted lines represent the time distributions of the events in radioactive decays [19] with half-lives of $T_{1/2}=1.09$ ms and $T_{1/2}=22$ μs. (b) The corresponding spectra for the α decay of the isomeric state in ^{171}Au. In the correlation, the α decay of ^{167}Ir^{m} is demanded as a daughter decay.

2(b) (The ^{171}Au^{m} α peak was used for the calibration, see Table I). The results are in good agreement with the α decay of the $11/2^{-}$ isomeric state with $E_{\alpha}=6996(6)$ keV and $T_{1/2}=1.02(10)$ ms reported in Ref. [2].

3. Decay scheme of ^{171}Au

Figure 4 shows the decay scheme obtained for ^{171}Au in the present work. The half-life of $T_{1/2}=1.09(3)$ ms for the $11/2^{-}$ isomeric state was obtained by combining the statistics of the proton emission and the α decay. The decay scheme agrees with the earlier results discussed in more detail in Refs. [2,9]. The data shown for ^{167}Ir are taken from Ref. [2].

The experimental spectroscopic factors $S^{\text{expt.}}$ shown in Fig. 4 and Table III were established based on a WKB approximation calculation through the real part of a Becchetti-Greenlees optical model potential [24]. The experimental spectroscopic factor of $S^{\text{expt.}}=0.23(7)$ was obtained for $\Delta\ell=0$ proton emission from the $1/2^{+}$ ground state in ^{171}Au. The value is in good agreement with the theoretical value of $S^{\text{calc}}=0.22$ predicted by the low-seniority shell model calculations for Au isotopes [2]. The present value is also consistent with the previous experimental result $S^{\text{expt.}}=0.26^{+0.14}_{-0.08}$ [9]. Correspondingly, the spectroscopic factor of $S^{\text{expt.}}=0.13(2)$ obtained for $\Delta\ell=5$ proton emission from the $11/2^{-}$ isomeric state is slightly lower than the theoretical prediction and the previous experimental value of $S^{\text{expt.}}=0.19(3)$ [2]. The major difference between the experimental spectroscopic factors originates from the slightly different proton and α decay branches of the $11/2^{-}$ state obtained in the present and the previous work. In the present analysis a branch of 0.8(1) for the α decay of the $11/2^{-}$ state in the daughter nucleus ^{167}Ir [2] was used. The α-decay hindrance factors, shown in Table IV, were determined according to the method of Rasmussen [25] and normalized to the α decay of ^{212}Po. The α decay of the $11/2^{-}$ isomeric state in ^{171}Au shows an unhindered $\Delta\ell=0$ character with a hindrance factor of 0.80(6). This is in agreement with the previous conclusion [2] that the spins and parities of the initial and the final states in the α decay of ^{171}Au^{m} to ^{167}Ir^{m} are the same.

The excitation energy of 258(13) keV for the $11/2^{-}$ state in ^{171}Au was determined using the proton emission Q values (based on the proton peaks used for the calibration, see Table II). The result is in good agreement with the previously established value, 250(16) keV [9].

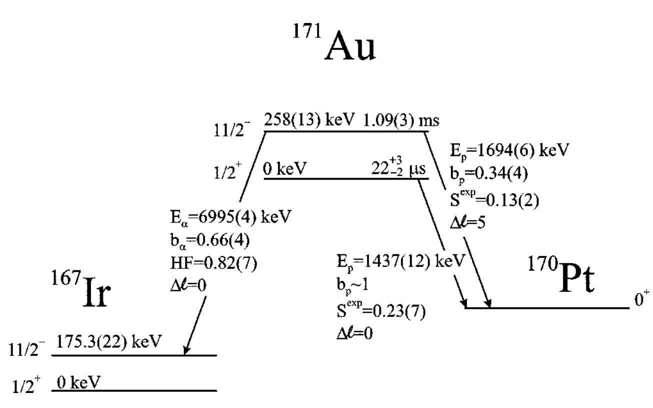

FIG. 4. Decay scheme of ^{171}Au. Data for ^{167}Ir are taken from Ref. [2].

TABLE III. Proton emission data obtained in the present work. The theoretical proton emission half-lives $T_{1/2}^{\mathrm{WKB}}$ were calculated using the WKB barrier transmission approximation with the real part of the optical model potential given by Becchetti and Greenlees [24]. The electron screening correction to the proton emission energy was taken from Ref. [35].

Nucleus	E_p (keV)	b_p	$T_{1/2}^{p}$	Proton orbital	$T_{1/2}^{\mathrm{WKB}}$	$S^{\mathrm{expt.}}$
				$s_{1/2}$	5.1 μs	0.23(7)
$^{171}\mathrm{Au}^{g}$	1437(12)	1	(22^{+3}_{-2}) μs	$d_{3/2}$	39.2 μs	1.8(6)
				$h_{11/2}$	63.4 ms	~2880
				$s_{1/2}$	36.3 ns	$\sim 1.1\times 10^{-5}$
$^{171}\mathrm{Au}^{m}$	1694(6)	0.34(4)	3.2(4) ms	$d_{3/2}$	271 ns	$\sim 8.5\times 10^{-5}$
				$h_{11/2}$	400.8 μs	0.13(2)
				$s_{1/2}$	3.0 μs	0.009(3)
$^{170}\mathrm{Au}^{g}$	1463(12)	0.89(10)	321(70) μs	$d_{3/2}$	22.9 μs	0.071(20)
				$h_{11/2}$	37 ms	115(40)
				$s_{1/2}$	16.3 ns	$\sim 1.5\times 10^{-5}$
$^{170}\mathrm{Au}^{m}$	1743(6)	0.58(5)	1064(100) μs	$d_{3/2}$	122 ns	$\sim 1.1\times 10^{-4}$
				$h_{11/2}$	180 μs	0.17(3)
				$s_{1/2}$	1.9 ns	$\sim 6.4\times 10^{-6}$
$^{177}\mathrm{Tl}^{m}$	1954(12)	0.55(20)	(290^{+150}_{-110}) μs	$d_{3/2}$	13 ns	$\sim 4.6\times 10^{-5}$
				$h_{11/2}$	16.1 μs	0.06(3)
				$s_{1/2}$	1.49 ms	0.29(20)
$^{176}\mathrm{Tl}^{g}$	1258(18)	~1	$(5.2^{+3.0}_{-1.4})$ ms	$d_{3/2}$	11.2 ms	2.2(15)
				$h_{11/2}$	17.5 s	~2400

TABLE IV. The measured α-decay properties. The hindrance factors and reduced widths are calculated from measured values by using the method of Rasmussen [25] and normalized to the α decay of ^{212}Po. In the calculation, the $\Delta\ell$ values were taken to be zero for each α decay. The α-decay properties taken from literature references are also shown for comparison. Half-lives are given in millisecond unless otherwise stated.

	E_α(keV)		$T_{1/2}$(ms)		$I_{\mathrm{rel.}}$(%)				
Nucleus	This work	Literature	This work	Literature	This work	Literature	Reference	HF	δ^2 (keV)
$^{177}\mathrm{Tl}^{m}$	7472(11)	7487(13)	$(160^{+70}_{-40})\mu$s	230(40)μs	45(20)	49(8)	[9]	$0.9^{+0.5}_{-0.4}$	70^{+40}_{-30}
^{171}Hg	7488(12)		$(59^{+36}_{-16})\mu$s					$0.4^{+0.3}_{-0.2}$	170^{+100}_{-50}
^{172}Hg	7361(14)	7350(12)	$0.32^{+0.32}_{-0.11}$	$0.25^{+0.35}_{-0.09}$			[29]	$0.9^{+1.0}_{-0.3}$	70^{+70}_{-30}
^{173}Hg	7192(13)	7211(11)	$0.59^{+0.47}_{-0.18}$	$0.93^{+0.57}_{-0.26}$			[29]	$0.5^{+0.4}_{-0.2}$	130^{+100}_{-40}
$^{170}\mathrm{Au}^{m}$	7107(6)		$(617^{+50}_{-40})\mu$s		42(5)			1.6(3)	40(6)
$^{170}\mathrm{Au}^{g}$	7001(10)		$(286^{+50}_{-40})\mu$s		11(10)			1.3(12)	51(48)
$^{171}\mathrm{Au}^{m}$	6995(4)	6996(6)	1.09(3)	1.02(10)	66(4)	54(4)	[2]	0.80(6)	80(6)
^{167}Pt	6979(7)	6988(10)	$0.9^{+0.3}_{-0.2}$	0.7(2)			[22]	$0.9^{+0.3}_{-0.2}$	80^{+30}_{-20}
^{168}Pt	6820(4)	6832(10)	2.1(2)	2.0(4)			[22]	0.61(7)	105(11)
^{169}Pt	6691(3)	6698(23)	7.0(2)	5(3)			[23]	0.79(6)	82(6)
^{170}Pt	6549(2)	6550(6)	14.0(2)	14.7(5)			[22]	0.51(4)	127(6)
$^{166}\mathrm{Ir}^{m}$	6545(4)	6561(5)	$14.3^{+1.9}_{-1.5}$	15.1(9)		98.24(58)	[2]	1.2(2)	55(10)
$^{166}\mathrm{Ir}^{g}$	6551(11)	6562(6)	17^{+12}_{-5}	10.1(22)		93.1(29)	[2]	$1.5^{+1.0}_{-0.5}$	45^{+30}_{-14}
$^{167}\mathrm{Ir}^{m}$	6394(2)	6410(5)	25.7(8)	30.2(20)		80(10)	[2]	0.62(3)	104(4)

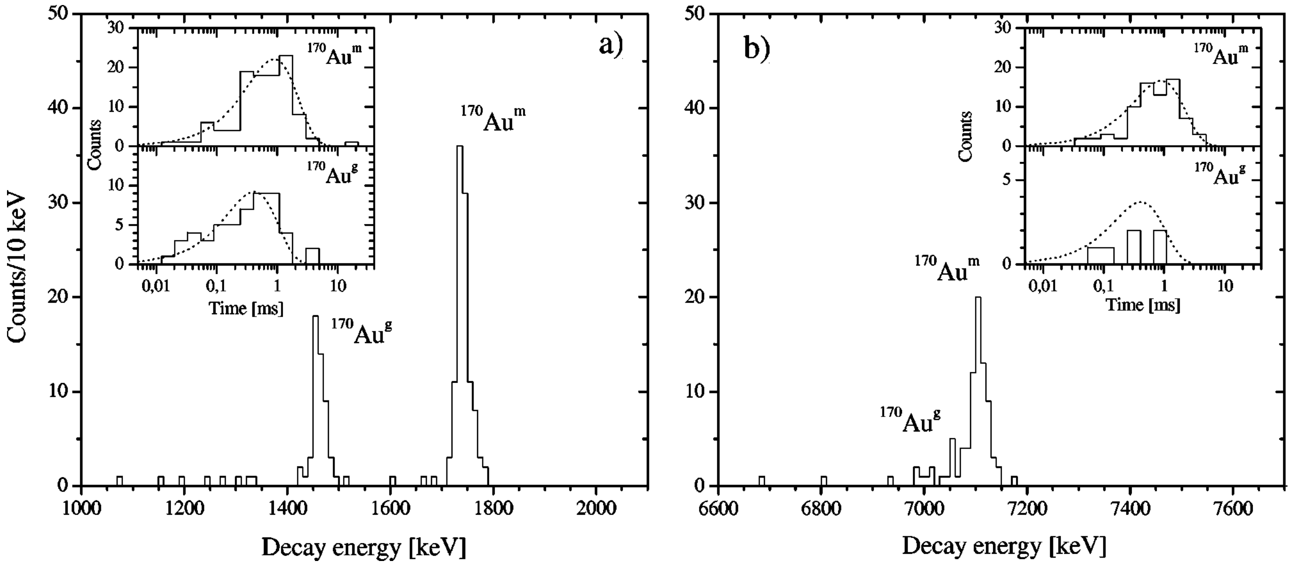

FIG. 5. Proton and α-particle energy spectra and time distributions for the decays of ^{170}Au. (a) The ER$-p_m-\alpha_d$ correlated proton energy spectrum for ^{170}Au where the α decay of ^{169}Pt is demanded as a daughter decay. Search times of 10 ms and 200 ms were used for mother and daughter decays, respectively. The time distributions of the ^{170}Au^m and ^{170}Au^g proton emissions in ER$-p_m-\alpha_d$ correlated decay chains are shown in the inset panel. For time distributions a longer search time of 50 ms was used for the mother activity. The dotted lines represent the time distributions of the events in radioactive decays [19] with a half-life of $T_{1/2}$=617 μs and $T_{1/2}$=286 μs for the isomeric and for ground-state decay, respectively. (b) The corresponding spectra for the α decays of ^{170}Au. In the correlation, the α decay of ^{166}Ir is demanded as a daughter decay.

C. The decay of ^{170}Au

1. The proton decay of ^{170}Au

Two states decaying by proton emission were assigned to ^{170}Au in Fig. 2(a). The identification was based on the ER $-p_m-\alpha_d$ correlated decay chains.

The daughter activities of group ^{170}Au^g and ^{170}Au^m in Fig. 2(a) were identified to originate from the decay of the ground state in ^{169}Pt. An α-decay energy of E_α =6691(4) keV and half-life $T_{1/2}=(6.5^{+0.7}_{-0.6})$ ms were determined from 104 ER$-p_m-\alpha_d$ correlated decay chains for the daughter activity of group ^{170}Au^m in Fig. 2(a). Correspondingly, an α-decay energy of E_α=6689(5) keV and half-life $T_{1/2}=(6.4^{+1.1}_{-0.8})$ ms were obtained from 50 ER$-p_m-\alpha_d$ correlated decay chains for the daughter activity of group ^{170}Au^g. The characteristics of both decays are in agreement with the α-decay properties of E_α=6698(23) keV and $T_{1/2}$=5(3) ms reported for ^{169}Pt [23]. By combining the statistics of both groups an α-decay energy of E_α=6690(4) keV and half-life $T_{1/2}=(6.5^{+0.6}_{-0.5})$ ms were obtained for ^{169}Pt.

A large number of ^{169}Pt nuclei were also produced directly in the present work as can be seen in Figs. 1(b) and 2(b). Based on ER$-\alpha_m$ and ER$-\alpha_m-\alpha_d$ correlated decay chains, starting with the α decay of ^{169}Pt, an α-decay energy of E_α=6691(3) keV and half-life $T_{1/2}$=7.0(2) ms were obtained for ^{169}Pt in agreement with previous results [23] (The ^{169}Pt α peak was used for the calibration, see Table I). In addition, the α-decay energy of E_α=6175(3) keV and half-life $T_{1/2}$=77(3) ms obtained for the daughter nucleus ^{165}Os are broadly consistent with the previous values E_α =6188(7) keV and $T_{1/2}$=71(3) ms [23].

Also the proton emission of ^{170}Au correlates directly with the α decay of the granddaughter nucleus ^{165}Os, as can be seen in Fig. 2(a). Using quadruple correlated full energy decay chains an α-decay energy of E_α=6178(5) keV and half-life $T_{1/2}$=80(20) ms were obtained for the granddaughter α decay. The values are in agreement with the results established for the α decay of ^{165}Os above and in Ref. [23].

A proton energy of E_α=1743(6) keV and half-life $T_{1/2}$ =(590^{+70}_{-60}) μs were established for the mother activity of group ^{170}Au^m in Fig. 2(a). The results are in good agreement with the previous experimental values of E_α=1735(9) keV and $T_{1/2}=(570^{+310}_{-150})$ μs [26]. Based on ER$-p_m-\alpha_d$ correlated decay chains a proton energy of E_α=1463(11) keV and half-life $T_{1/2}=(283^{+50}_{-40})$ μs were obtained for the mother activity of group ^{170}Au in Fig. 2(a). Further discussion about the decay scheme is given later in Sec. III C 3.

Figure 5(a) shows the ER$-p_m-\alpha_d$ correlated proton energy spectrum for ^{170}Au demanding the α decay of ^{169}Pt as a daughter decay (α-decay energy between 6630 keV and 6750 keV). The time distributions of the proton emissions in ER$-p_m-\alpha_d$ correlated decay chains for ^{170}Au^m and ^{170}Au^g are shown in the inset panels of Fig. 5(a). Figure 5(b) shows the corresponding spectra for the α decay of ^{170}Au. In these correlations the α decay of ^{166}Ir is demanded as a daughter decay (α-decay energy between 6510 keV and 6580 keV).

2. The α decay of ^{170}Au

Two α-decaying states were assigned to ^{170}Au in Fig. 2(b). Identification of the mother decays was based on ER $-\alpha_m-\alpha_d$ correlated decay chains, where the previously known α decays of ^{166}Ir were observed as the daughter decay. In order to distinguish the isomeric and the ground-state α decays, longer decay chains were also searched for. The final connections between the proton-emitting and the

α-decaying states in ^{170}Au were based on the half-life and the Q-value examination to be discussed later in Sec. III C 3.

The daughter activity of group ^{170}Au^m in Fig. 2(b) was identified to originate from the isomeric high-spin state in ^{166}Ir. An α-decay energy of $E_\alpha = 6545(4)$ keV and half-life $T_{1/2} = (14.3^{+1.9}_{-1.5})$ ms were determined from 75 ER$-\alpha_m-\alpha_d$ correlated decay chains. The decay properties are broadly consistent with the previous results reported with $E_\alpha = 6561(5)$ keV and $T_{1/2} = 15.1(9)$ ms [2]. In addition, the mother α decay of group ^{170}Au^m correlates directly with the α decay of the granddaughter and even the great-granddaughter nuclei ^{162}Re^m and ^{158}Ta^m, respectively [see Fig. 2(b)]. Based on the quadruple-correlated full-energy decay chains, an α-decay energy of $E_\alpha = 6112(5)$ keV and half-life $T_{1/2} = (74^{+15}_{-10})$ ms were obtained for the third generation α decay of group ^{170}Au^m. The results are in good agreement with the values of $E_\alpha = 6116(5)$ keV and $T_{1/2} = 84.6(62)$ ms given for the α decay of ^{162}Re^m [2]. In addition, the α-decay energy of $E_\alpha = 6048(7)$ keV obtained for the decay of ^{158}Ta^m is in good agreement with the previous experimental result $E_\alpha = 6048(5)$ keV [2].

An α-decay energy of $E_\alpha = 7107(6)$ keV and half-life $T_{1/2} = (655^{+90}_{-70})$ μs were established for the mother decay of group ^{170}Au^m in Fig. 2(b) based on ER$-\alpha_m-\alpha_d$ correlated decay chains. Justification for the assignment to an isomeric state is discussed later in Sec. III C 3.

An α-decay energy of $E_\alpha = 6551(11)$ keV and half-life $T_{1/2} = (17^{+12}_{-5})$ ms were determined from 6 ER$-\alpha_m-\alpha_d$ correlated decay chains for the daughter activity of group ^{170}Au^g in Fig. 2(b). The decay properties are broadly consistent with the α decay of the ground state in ^{166}Ir reported with $E_\alpha = 6562(6)$ keV and $T_{1/2} = 10.1(22)$ ms in Ref. [2]. In addition, two of the correlated triple chains were correlated with third generation α decays of the granddaughter nucleus ^{162}Re. The observed α-decay energy of $E_\alpha = 6081(17)$ keV and half-life $T_{1/2} = (120^{+300}_{-50})$ ms are consistent with the previous results $E_\alpha = 6086(5)$ keV and $T_{1/2} = 107(13)$ ms [2] reported for the ground-state α decay of ^{162}Re.

An α-decay energy of $E_\alpha = 7001(10)$ keV and half-life $T_{1/2} = (310^{+220}_{-90})$ ms were obtained for the mother activity of group ^{170}Au^g in Fig. 2(b). Based on the decay chain and the discussion in Sec. III C 3 the mother activity is concluded to originate from the ground state of ^{170}Au.

3. Decay scheme of ^{170}Au

Figure 6 shows the decay scheme obtained for ^{170}Au in the present work. The data shown for ^{166}Ir are taken from Ref. [2].

As discussed in the previous sections, two proton emitting and α-decaying states were identified for the ^{170}Au nucleus. Both of the proton radioactivities were observed to feed the ground state of ^{169}Pt. Based on this observation, it is concluded that the proton emission with an energy of $E_p = 1463(12)$ keV originates from the ground state of ^{170}Au. Correspondingly, based on the Q-values, the proton emission with $E_p = 1743(6)$ keV was assigned to originate from an isomeric state at 282(10) keV in ^{170}Au.

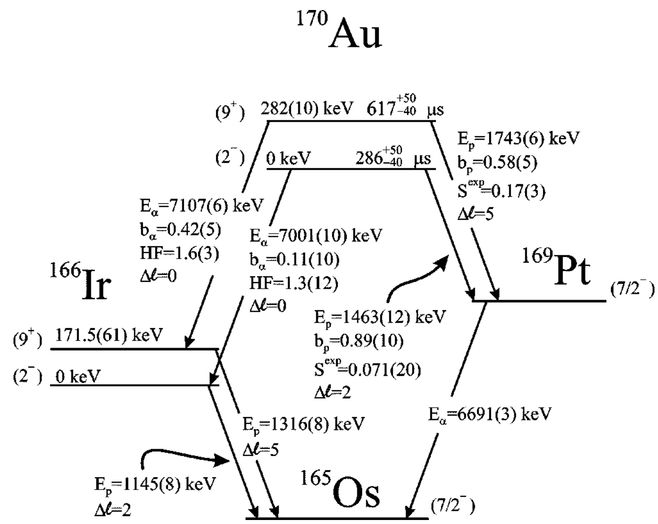

FIG. 6. Decay scheme of ^{170}Au. Data shown for ^{166}Ir are taken from Ref. [2].

Among the α decays, a state with an α-decay energy of $E_\alpha = 7107(6)$ keV was observed with a half-life consistent with the proton radioactivity of the isomeric state with $E_p = 1743(6)$ keV. Correspondingly, the half-life of the weak α-decay branch with $E_\alpha = 7001(10)$ keV is in good agreement with the half-life of the ground-state proton emission with $E_p = 1463(12)$ keV. In addition, the decay chains starting with the $E_\alpha = 7107(6)$ keV and $E_\alpha = 7001(10)$ keV α decays were observed to feed the isomeric and the ground state, respectively, in the daughter nucleus ^{166}Ir. Further, the isomeric and the ground-state decay chains can be clearly distinguish based on the decay properties of the granddaughter nucleus ^{162}Re.

Using the measured Q-values for the proton emission of ^{170}Au and ^{166}Ir [2] and for the α decay of ^{169}Pt, it is possible to estimate the α-decay energies of the ground state and the isomeric state in ^{170}Au. The resulting α-decay energies of 7004(15) keV between the ground states and 7111(11) keV between the isomeric states in ^{170}Au and ^{166}Ir are in good agreement with the observed α-decay energies.

Consequently, the α decay with an energy of $E_\alpha = 7001(10)$ keV and proton emission with $E_p = 1463(12)$ keV are concluded to originate from the ground state of ^{170}Au. Combining the statistics of the proton emission and α decay a half-life of $T_{1/2} = (286^{+50}_{-40})$ μs was obtained for the decay of the ground state. Taking into account the number of ER$-p_m/\alpha_m-\alpha_d$ correlated decay chains and branches in the daughter nuclei **[**$b_\alpha = 0.931(29)$ for the ground state in ^{166}Ir [2]**]** α decay and proton emission branches of $b_\alpha = 0.11(10)$ and $b_p = 0.89(10)$, respectively, were obtained for the ground-state decay of ^{170}Au.

Correspondingly, the α decay with $E_\alpha = 7107(6)$ keV was concluded to originate from the isomeric state at 282(10) keV along with the $E_p = 1743(6)$ keV proton emission. Combining the statistics of the proton emission and the α decay, a half-life of $T_{1/2} = (617^{+50}_{-40})$ μs was obtained for the decay of the isomeric state in ^{170}Au. Based on the number of ER$-p_m/\alpha_m-\alpha_d$ correlated decay chains the branches of b_α

$=0.41(6)$ and $b_{\mathrm{p}}=0.59(6)$ were obtained for the decay of the isomeric state. An α-decay branch of $b_{\alpha}=0.9824(58)$ for the isomeric state in the daughter nucleus ^{166}Ir [2] was taken into account.

Table III shows the results obtained for the proton emission of ^{170}Au. The experimental partial half-lives of the proton emissions are compared to the WKB approximated half-lives $T_{1/2}^{\mathrm{WKB}}$ for a proton emission from $s_{1/2}$, $d_{3/2}$, and $h_{11/2}$ orbitals.

The low-seniority shell-model calculation introduced in Ref. [2] predicts that the spectroscopic factor S^{calc} for proton emission in Au isotopes is 0.22. Comparing the measured and calculated proton half-lives in Table III the ground-state proton emission in ^{170}Au can be explained with the $\Delta\ell=2$ transition. This indicates that the proton is emitted from the $\pi d_{3/2}$ orbital similarly as observed for the ground-state proton emission in the α-decay daughter nucleus ^{166}Ir [2]. The experimental spectroscopic factor of $S^{\mathrm{expt.}}=0.071(20)$ for the ground-state proton emission in ^{170}Au is a little lower that the calculated value $S^{\mathrm{calc}}=0.22$, but this is typical for the $d_{3/2}$ proton emission. It has been observed that the one-dimensional semiclassical WKB approximation which works well for the proton emission from $s_{1/2}$ and $h_{11/2}$ orbitals, underestimates the half-life for the proton emission from the $d_{3/2}$ orbital. The proton emission from the $d_{3/2}$ orbital is successfully described by a particle-vibration coupling model approach introduced in Refs. [27,28].

The proton emission from the isomeric state in ^{170}Au can be explained by a $\Delta\ell=5$ transition corresponding to proton emission from the $\pi h_{11/2}$ orbital. This indicates that also the structure of the isomeric state in ^{170}Au is similar to the isomeric state in the α-decay daughter nucleus ^{166}Ir [2]. The experimental spectroscopic factor of $S^{\mathrm{expt.}}=0.17(3)$ for the isomeric proton emission is in agreement with the theoretical prediction as well as the previous experimental result $S^{\mathrm{expt.}}\sim 0.21$ [26].

The α-decay hindrance factors for ^{170}Au are shown in Fig. 6 and Table IV. The hindrance factors of 1.3(12) and 1.6(3) obtained for the α decay of the ground state and the isomeric state, respectively, reveal their unhindered character. This is in agreement with the conclusions based on the proton emission discussed above that the structures of the ground states and the isomeric states, respectively, in ^{170}Au and the α-decay daughter nucleus ^{166}Ir are similar. Thus, based on the configurations given for ^{166}Ir in Ref. [2], $[\pi d_{3/2}\nu f_{7/2}]_{2^-}$ and $[\pi h_{11/2}\nu f_{7/2}]_{9^+}$ configurations can be suggested for the ground state and the isomeric state, respectively, in ^{170}Au.

The proton emissions and the proton-neutron configurations in ^{170}Au can be used to deduce the spin and parity of the ground state in the daughter nucleus ^{169}Pt. If it is assumed that the $\nu f_{7/2}$ neutron orbital characterizes the states observed in ^{170}Au, the same orbital represents the neutron configuration in the daughter nucleus. This would lead to the spin and parity assignment of $7/2^-$ for the ground state in ^{169}Pt. This tentative result is consistent with the $7/2^-$ assignment of the ground state in ^{165}Os [2]. The spins and parities of the ground states of these nuclei have to be the same, since the states are connected by an unhindered α decay (see Table IV). The preliminary spin and parity assignments are shown in Fig. 6.

D. The α decay of ^{171}Hg and ^{172}Hg

A new α-decaying isotope ^{171}Hg and the previously known ^{172}Hg isotope [29] were produced via 3n- and 2n-fusion evaporation channels in the bombardment of the ^{96}Ru target with the ^{78}Kr ion beam. The identification of the isotopes, shown in Fig. 2(b), was based on ER$-\alpha_{\mathrm{m}}-\alpha_{\mathrm{d}}$ correlated decay chains where the α decays of the corresponding daughter nuclei ^{167,168}Pt or granddaughter nuclei ^{163,164}Os were observed to follow the mother α decay. Since the ^{167}Pt and ^{168}Pt isotopes were also produced directly in the present experiment their decay properties were first established more precisely using the decay chains marked for them in Fig. 2(b).

Based on 134 ER$-\alpha_{\mathrm{m}}-\alpha_{\mathrm{d}}$ correlated decay chains an α-decay energy of $E_{\alpha}=6820(4)$ keV and half-life $T_{1/2}=2.1(2)$ ms were obtained for the mother decay and $E_{\alpha}=6310(3)$ keV and $T_{1/2}=(21.5^{+2.0}_{-1.7})$ ms for the daughter decay of the group ^{168}Pt in Fig. 2(b). The results are comparable with the previous experimental values $E_{\alpha}=6832(10)$ keV and $T_{1/2}=2.0(4)$ ms for ^{168}Pt and $E_{\alpha}=6315(10)$ keV and $T_{1/2}=27(4)$ ms for ^{164}Os reported in Ref. [22]. Also in Ref. [23] comparable values of $E_{\alpha}=6321(7)$ keV and $T_{1/2}-21(1)$ ms are reported for the α decay of ^{164}Os.

An α-decay energy of $E_{\alpha}=6979(7)$ keV and half-life $T_{1/2}=(0.9^{+0.3}_{-0.2})$ ms were obtained for the mother decay of the group ^{167}Pt in Fig. 2(b). For the corresponding daughter activity an α-decay energy of $E_{\alpha}=6496(6)$ keV and half-life $T_{1/2}=(9.3^{+2.2}_{-1.5})$ ms were established. The analysis is based on 27 ER$-\alpha_{\mathrm{m}}-\alpha_{\mathrm{d}}$ correlated decay chains. The results are broadly consistent with the previous experimental values of $E_{\alpha}=6988(10)$ keV and $T_{1/2}=0.7(2)$ ms for ^{167}Pt and $E_{\alpha}=6514(10)$ keV and $T_{1/2}=5.5(6)$ ms for ^{163}Os reported in Ref. [22]. In addition, in Ref. [23] comparable values are reported for the α decay of ^{163}Os with $E_{\alpha}=6512(19)$ keV and $T_{1/2}=(12^{+11}_{-7})$ ms.

One triple-correlated full-energy α-decay chain and three triple-correlated α-decay chains where the α particle from the daughter decay has escaped the silicon detector were observed for ^{172}Hg in Fig. 2(b). The α-decay properties of the daughter nucleus and the α-decay energy of the granddaughter nuclei were observed to agree with the decay properties of ^{168}Pt and ^{164}Os obtained above.

Based on the decay chains an α-decay energy of $E_{\alpha}=7361(14)$ keV and half-life $T_{1/2}=(320^{+320}_{-110})$ μs were established for ^{172}Hg. The results are in good agreement with the previous experimental result with $E_{\alpha}=7350(12)$ keV and $T_{1/2}=(250^{+350}_{-90})$ μs [29]. The event with a daughter α-decay energy of approximately 6000 keV in Fig. 2(b) is not taken into account in the analysis, since the lifetime of the mother decay in this decay chain is approximately thirteen times longer than the lifetimes of the mother activities in the other decay chains. In addition, the energy of the daughter α decay does not agree with the known α decays existing in the decay chain starting with the α decay of ^{172}Hg.

Three triple-correlated full energy α-decay chains were observed for a new α-active isotope ^{171}Hg in Fig. 2(b). In addition, two α decays, most likely originating from ^{171}Hg, were observed to correlate directly with the granddaughter (^{163}Os) α decay. The decay chain where the α-decay energy of the daughter activity is approximately 6450 keV was not taken into account in the analysis since the half-life of the mother decay is on the order of hundred times longer than the half-life of the mother decays in the other decay chains. Two more α-decay events with a decay energy and a half-life consistent with the ^{171}Hg events in the correlated decay chains mentioned above were observed to correlate only with the preceding recoil. By taking into account all these seven events an α-decay energy of $E_\alpha = 7488(12)$ keV and half-life $T_{1/2} = (59^{+36}_{-16})$ μs were obtained for the decay of the ^{171}Hg isotope.

The hindrance factors and reduced widths for the α decays of ^{171}Hg and ^{172}Hg were calculated and are shown in Table IV. The values indicate that both of the α decays can be associated with an unhindered $\Delta\ell = 0$ transition.

E. Cross sections in the reaction ^{78}Kr + ^{96}Ru

In the following a transmission of 40% was used for the RITU separator and the bombarding energies are given in the middle of the target.

For ^{171}Au the highest total production cross section of approximately 1.1 μb was obtained at the lowest bombarding energy of 361 MeV. This corresponds to a compound nucleus ^{174}Hg excitation energy of approximately 46 MeV. The cross section is comparable with the previous values of 2 μb and 0.6 μb at the bombarding energies of 359 MeV and 363 MeV, respectively [2,21]. For ^{170}Au the maximum cross section of approximately 90 nb was obtained at a bombarding energy of 386 MeV.

Since the ^{171}Hg and ^{172}Hg isotopes were obtained as side products of the experiment the bombarding energies were not optimized for them. Thus, the maximum production cross sections were not necessarily reached. For ^{172}Hg a production cross section of approximately 4 nb was measured at the lowest bombarding energy of 361 MeV. In Ref. [29] a cross section of 9 nb was measured applying the same ^{78}Kr + ^{96}Ru reaction but using 10 MeV lower excitation energy of the compound nucleus. Thus, the maximum production yield for the ^{172}Hg isotope was not reached in the present work. For the production of ^{171}Hg the highest cross section of approximately 2 nb was obtained at the lowest bombarding energy. Since the excitation energy of the compound nucleus was only 10 MeV higher than the optimum energy for the production of ^{172}Hg in the 2n channel [29] the optimum bombarding energy for the production of the ^{171}Hg isotope in the 3n channel cannot differ too much from the one used.

F. Reaction ^{78}Kr + ^{102}Pd

The energy spectrum of all decay events from the ^{78}Kr + ^{102}Pd reaction observed in the silicon detector and vetoed with the gas counter and the punch-through detectors is shown in Fig. 7(a). The spectrum is dominated by activities

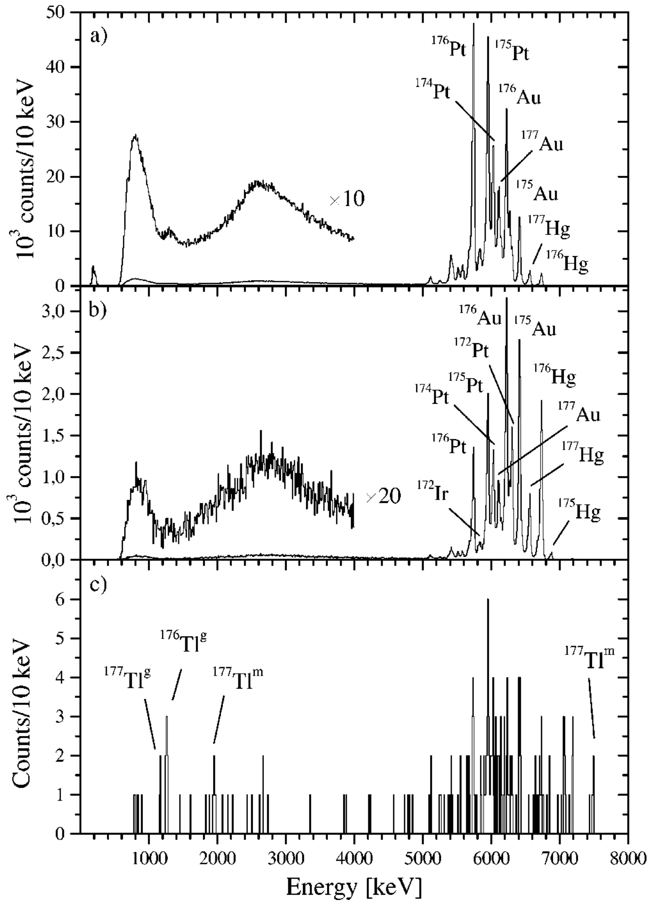

FIG. 7. (a) Energy spectrum observed in the silicon detector and vetoed with the gas counters and punch though detectors in the reaction ^{78}Kr + ^{102}Pd. (b) The same data after requiring a position and time correlation with the implanted evaporation residues within a search time of 50 ms and (c) with an additional requirement of subsequent α decay in the same position within a 500 ms search time and with a decay energy between 6500–7000 keV.

produced in fusion-evaporation channels involving an evaporation of charged particles. As in the ^{78}Kr + ^{96}Ru experiment, the effect of the vetoed escaped α particles is clearly visible in Fig. 7(a). Figure 7(b) shows the same data after requiring a position and time correlation with the preceding recoil event within a search time of 50 ms. Figure 7(c) shows the data after a further requirement that the decay is followed by an α decay in the same position, within a search time of 500 ms and with an α-decay energy between 6500 keV and 7000 keV. The decay peaks of the evaporation products of the $p2n$- and $p3n$-channels, ^{177}Tl and ^{176}Tl, respectively, are visible in the spectrum. The final identification of the previously known isotope ^{177}Tl [9] and a new proton-emitting nucleus ^{176}Tl were based on the ER$-p_\mathrm{m}/\alpha_\mathrm{m}-\alpha_\mathrm{d}$ correlated decay chains shown in the two-dimensional mother and daughter decay energy plots in Figs. 8(a) and 8(b). In the plots the maximum search times of 50 ms and 500 ms were used for the mother and daughter decays, respectively.

G. The decay of ^{177}Tl

A few decay chains originating from the decay of the isomeric state in ^{177}Tl were observed in the present work.

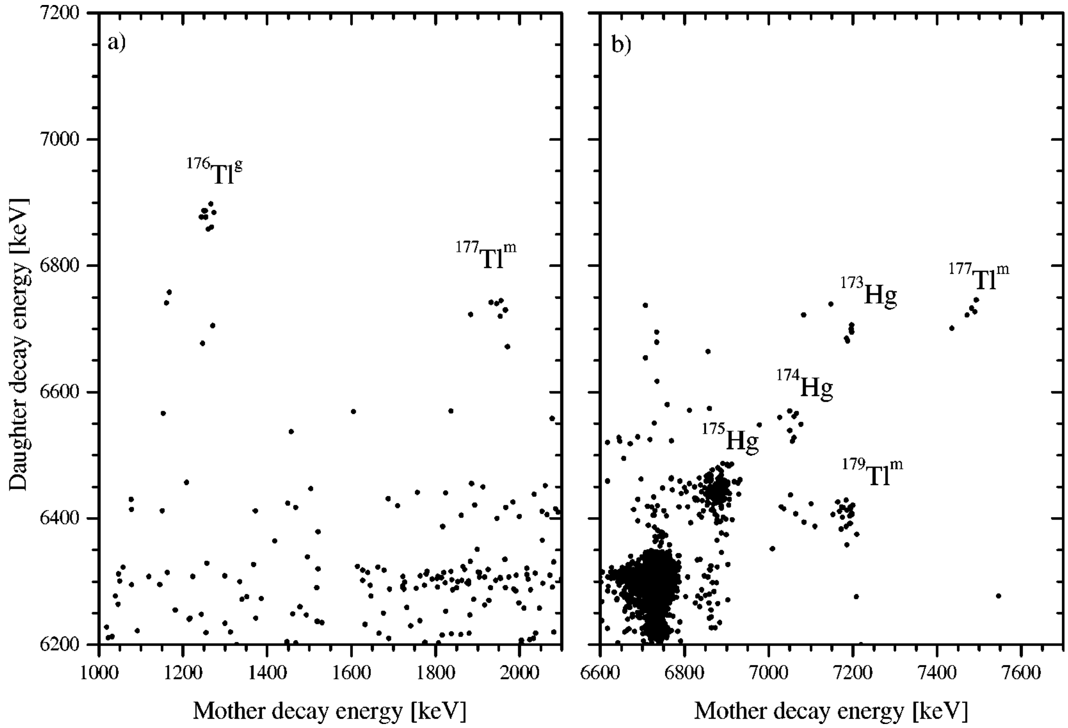

FIG. 8. Two-dimensional plot of the mother and daughter decay energies of ER$-p_m/\alpha_m-\alpha_d$ correlated decay chains observed in the ^{78}Kr+^{102}Pd reaction. (a) Shows the correlations where the proton emission of mother nuclei is followed by an α decay of the daughter nuclei (ER$-p_m-\alpha_d$). (b) Shows the correlated α-decay chains (ER$-\alpha_m-\alpha_d$). Maximum search times for the mother and daughter decays were 50 ms and 500 ms, respectively.

The decay chains starting with either a proton or an α decay are identified in Figs. 8(a) and 8(b). The identification was based on the ER$-p_m/\alpha_m-\alpha_d$ correlated decay chains where the α decays of ^{176}Hg or ^{173}Au^m were observed to follow the parent proton and α decay, respectively. For an additional confirmation the granddaughter decays were also searched for. It should be noted that this part of the experiment was dedicated to the production of ^{176}Tl and the ^{177}Tl isotope was obtained as a side product. Thus the statistics for ^{177}Tl is limited and the identification of the ground-state decay was not attempted.

1. The proton decay of ^{177}Tl

An α-decay energy of $E_\alpha=6725(10)$ keV and half-life $T_{1/2}=(19^{+13}_{-6})$ ms were obtained for the daughter activity of group ^{177}Tl^m in Fig. 8(a). The results are broadly consistent with the previous values of $E_d=6750(20)$ keV and $T_{1/2}=18(10)$ ms reported for ^{176}Hg [23]. In addition, three of the decay chains were correlated with the granddaughter decay showing an α-decay energy of $E_\alpha=6313(14)$ keV and half-life $T_{1/2}=(100^{+130}_{-40})$ ms consistent with the decay properties of $E_\alpha=6314(4)$ keV and $T_{1/2}=96(3)$ ms given for ^{172}Pt in Refs. [23,30].

The mother decay was identified as proton emission from the isomeric state in ^{177}Tl. Thus, the proton line was used for the proton energy calibration of the experiments as given in Table II. The decay properties of the mother activity with an energy of $E_p=1954(12)$ keV and a half-life of $T_{1/2}=(210^{+150}_{-60})$ μs are consistent with the previous results $E_p=1958(10)$ keV and $T_{1/2}=230(40)$ μs reported for ^{177}Tl^m [9]. In the analysis the event with the mother decay energy of approximately 1880 keV close to the group was not taken into account since the decay time of the mother activity is approximately 150 times longer than that of the others in the group.

2. The α decay of ^{177}Tl

The daughter activity of the group ^{177}Tl^m in Fig. 8(b) was identified to originate from the α decay of the isomeric state in ^{173}Au. The present results with $E_\alpha=6725(11)$ keV and $T_{1/2}=(12^{+10}_{-4})$ ms agree with the previous results $E_\alpha=6732(4)$ keV and $T_{1/2}=(12^{+3}_{-2})$ ms given for ^{173}Au^m [9]. In addition, two of the decay chains were correlated with the granddaughter activity, consistent with the decay properties of the isomeric state in ^{169}Ir [9]. Based on the decay chain it was concluded that the mother activity of the group originates from the α decay of the isomeric state in ^{177}Tl. The α-decay energy of $E_\alpha=7472(11)$ keV observed in the present work is broadly consistent with the previous result $E_\alpha=7487(13)$ keV [9]. On the other hand, the half-life of $T_{1/2}=(95^{+80}_{-30})$ μs obtained for the decay is somewhat shorter than the corresponding half-life obtained from the proton emission above and given in Ref. [9]. However, since the other properties of the decay chain correspond to the previous results it was concluded that the mother decay does indeed originate from the α decay of the isomeric state in ^{177}Tl.

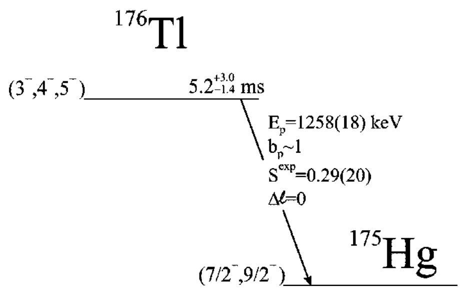

FIG. 9. Decay scheme for ^{176}Tl.

3. Spectroscopic and hindrance factors for ^{177}Tl^m

By combining the statistics obtained from the proton emission and the α decay, a half-life of $T_{1/2}=(160^{+70}_{-40})$ μs was obtained for the isomeric state in ^{177}Tl. Using the number of correlated decay chains branches of $b_\alpha=0.45(20)$ and $b_p=0.55(20)$ were derived for the α decay and the proton emission, respectively. The experimental spectroscopic factors $S^{\text{expt.}}$ for the proton emission are shown in Table III. Based on the results it is concluded that the proton emission corresponds to a $\Delta\ell=5$ transition from the $\pi h_{11/2}$ orbital as concluded earlier in Ref. [9]. The experimental spectroscopic factor obtained in the present work $S^{\text{expt.}}=0.06(3)$ is consistent with the previous experimental result $S^{\text{expt.}}=0.034(10)$ [9]. However, both of the results are somewhat lower than the theoretical value 0.11 predicted by a low-seniority shell-model calculation [2]. A more detailed discussion of the experimental spectroscopic factors in ^{177}Tl is presented in Ref. [9] (see also Sec. III H 2). The hindrance factor and the reduced width for the α decay (see Table IV) indicate an unhindered $\Delta\ell=0$ character for the transition.

H. The decay of ^{176}Tl

1. The proton decay of ^{176}Tl

Based on the properties of eight ER$-p_m-\alpha_d$ correlated decay chains in Fig. 8(a), the daughter activity of group ^{176}Tl^g was identified to originate from the α decay of ^{175}Hg. The observed α-decay energy of $E_\alpha=6880(10)$ keV and half-life $T_{1/2}=(7^{+4}_{-2})$ ms are comparable with the previous experimental results $E_\alpha=6897(11)$ keV and $T_{1/2}=(13^{+6}_{-4})$ ms [31]. A decay energy of $E_p=1258(18)$ keV and half-life $T_{1/2}=(5.2^{+3.0}_{-1.4})$ ms were established for the corresponding mother activity. Based on the properties of the decay chains the mother activity is concluded to originate from the proton emission of ^{176}Tl to the ground state of ^{175}Hg.

2. Decay scheme of ^{176}Tl

Figure 9 shows the decay scheme obtained for the decay of ^{176}Tl in the present work. Only one decay branch was identified. The experimental proton half-life is compared to calculated proton half-lives $T_{1/2}^{\text{WKB}}$ for the proton emission from $s_{1/2}$, $d_{3/2}$, and $h_{11/2}$ proton orbitals in Table III.

The low-seniority shell-model calculation [2] predicts that the spectroscopic factor S^{calc} for a proton emission in Tl isotopes is 0.11 when near degeneracy between $s_{1/2}$, $d_{3/2}$, and $h_{11/2}$ proton orbitals is assumed. Thus the proton half-lives calculated using the WKB approximation should be shorter than the measured values. However, the assumption of nearly degenerate orbitals does not necessarily hold in the case of light thallium isotopes. This is because the energy difference between the low- and high-spin states associated with $s_{1/2}$ and $h_{11/2}$ proton orbitals, respectively, is quite large. For example in the lightest previously known thallium isotope ^{177}Tl, the energy difference between the states is approximately 800 keV [9].

Based on the experimental spectroscopic factors presented in Table III the proton emission observed for ^{176}Tl most likely originates from the $s_{1/2}$ proton orbital. Thus, the observed proton emission represents the decay of the low-spin state which can be associated with the ground-state configuration in light thallium isotopes.

No α-decay branch was observed for ^{176}Tl. The α energy of the ground-state decay can be estimated using the observed proton energy and the mass information available for ^{175}Hg and ^{172}Au [32] (see also the mass excess examination in Sec. IV). The estimated α-decay energy of 7170(450) keV corresponds to a 3.1 ms half-life assuming an unhindered $\Delta\ell=0$ transition to the ground state of ^{172}Au. This suggests that the proton emission and the α decay from the ground state of ^{176}Tl should show almost equal strengths. However, the half-life estimate for ^{176}Tl is not accurate due to the uncertainties in the mass information. In addition, the ground-state α decay of ^{176}Tl may feed an excited state in ^{172}Au, which would lengthen the partial half-life of α decay.

The high-spin state should be fed more strongly than the low-spin state in the heavy ion fusion reaction. However, the decay of a possible high-spin state in ^{176}Tl where the proton can be expected to be emitted from an $h_{11/2}$ orbital was not observed. The reason is most probably the half-life which is too short to be detected with the data acquisition system used in the present experiment. In addition, a possibility of γ-ray deexcitation of the state cannot be excluded.

By taking into account the dead time of the data acquisition system (approximately 15 μs) it is possible to estimate the lowest limit for the excitation energy of the high-spin state. Since no proton emission was observed from an $h_{11/2}$ proton orbital it can be estimated that the half-life of the state should be at least three times shorter than the dead time. Based on the WKB approximation the lowest limit for the excitation energy of the high-spin state (proton emission from an $h_{11/2}$ orbital) is approximately 950 keV, when a 5 μs upper limit for the half-life and a spectroscopic factor of 0.11 were assumed. The estimated lower limit for the excitation energy is in agreement with the excitation energy observed for ^{177}Tl [9].

The observation of the ground-state proton emission from an $s_{1/2}$ orbital in ^{176}Tl differs from that observed for the lighter odd-odd proton emitting nuclei ^{156}Ta [11], ^{160}Re [12], ^{166}Ir [2], and ^{170}Au (Sec. III C 3). In these nuclei the ground-state proton emission has been deduced to occur from a $d_{3/2}$ proton orbital which was suggested to be coupled to an $f_{7/2}$ neutron. In ^{176}Tl$_{95}$ there are two orbitals $\nu f_{7/2}$ and $\nu h_{9/2}$, available for the odd neutron. By coupling these neutrons with a proton in the $\pi s_{1/2}$ orbital the $[\pi s_{1/2}\nu f_{7/2}]_{3^-,4^-}$ and $[\pi s_{1/2}\nu h_{9/2}]_{4^-,5^-}$ configurations are obtained, respectively.

Since the coupling properties of the odd proton and the odd neutron in such neutron-deficient Tl isotopes are not very well known, no definitive conclusion about the ground-state spin and parity assignment could be drawn based on the present data. However, the change in the ground-state proton configuration in ^{176}Tl compared to the lighter odd-odd proton emitters may indicate that the $\nu h_{9/2}$ orbital plays a role in the ground state of ^{176}Tl.

The proton emission of ^{176}Tl can be used to estimate the possible spin and parity assignment of the ground state of the daughter nucleus ^{175}Hg. If $[\pi s_{1/2}\nu f_{7/2}]_{3^-,4^-}$ or $[\pi s_{1/2}\nu h_{9/2}]_{4^-,5^-}$ configuration is assumed for the ground state in ^{176}Tl the odd neutron in the $f_{7/2}$ or $h_{9/2}$ orbital gives the assignment of $7/2^-$ or $9/2^-$, respectively, for the ground state of ^{175}Hg. The suggested configurations are consistent with the tentative level scheme of ^{177}Hg [33], where a $7/2^-$ assignment is suggested for the ground state and $9/2^-$ for a low-lying excited state at 77 keV. The tentative spin and parity assignments of the ground states in ^{176}Tl and ^{175}Hg are also shown in Fig. 9.

I. The α-decay of ^{173}Hg

Five ER$-\alpha_m-\alpha_d$ correlated decay chains were observed to originate from the α decay of ^{173}Hg in Fig. 8. The α-decay energy of $E_\alpha=7192(13)$ keV and half-life $T_{1/2}=(590^{+480}_{-180})$ μs obtained in the present work are broadly consistent with the previous experimental results $E_\alpha=7211(11)$ keV and $T_{1/2}=(930^{+570}_{-260})$ μs [29]. The α-decay properties of the subsequent daughter activity with $E_\alpha=6693(11)$ keV and $T_{1/2}=(13^{+11}_{-4})$ ms are broadly consistent with the α decay of ^{169}Pt (see Sec. III C 2 and Table IV) confirming the identification of ^{173}Hg.

The hindrance factor and reduced width of the α decay are shown in Table IV. The values are consistent with an unhindered $\Delta\ell=0$ transition.

J. Cross sections in the reaction ^{78}Kr+^{102}Pd

A maximum production cross section of approximately 3 nb was obtained for the ^{176}Tl isotope at a bombarding energy of 384 MeV in the middle of the target (40% transmission was assumed for RITU). The previously known isotope ^{173}Hg [29] was produced via the $\alpha 3n$ evaporation channel, as a side product of the thallium experiment. Assuming a lower 20% transmission for the αxn channels a production cross section of approximately 4 nb was obtained at a bombarding energy of 384 MeV in the middle of the target. This value is somewhat lower than the 15 nb cross section which was measured using the more favorable 3n-channel in reaction ^{80}Kr+^{96}Ru [29].

IV. MASS EXCESSES

Mass excesses for the ^{176}Tl, ^{171}Hg, and ^{170}Au nuclei were established based on the decay data obtained in the present work and the mass information available for the corresponding daughter nuclei. A mass excess of −8000(320) keV was given for ^{175}Hg in the recent mass evaluation of Audi *et al.* in Ref. [32]. Combining this value with the proton emission Q value measured for ^{176}Tl, a mass excess of 550(320) keV was obtained for ^{176}Tl. In Ref. [22] a mass excess of −7140(600) keV was derived for ^{167}Pt. This value leads to a mass excess of 2950(600) keV for ^{171}Hg. A mass excess of −12 650(310) is given for ^{169}Pt in Ref. [32]. Combining this value with the ground-state proton emission Q value a mass excess of −3870(310)keV is deduced for ^{170}Au.

V. SUMMARY

In the present work the decay properties of neutron-deficient Pt, Au, Hg, and Tl nuclei were measured. For the proton-emitting ^{170}Au nucleus, the ground-state proton emission and the α decay were observed for the first time, and the decay properties of the isomeric state were measured with improved accuracy. The decay of the proton-emitting ^{171}Au nucleus was used for the energy calibration and measured with high statistics. In mercury isotopes the α decay of a new isotope ^{171}Hg was observed and the decay properties of the previously known ^{172}Hg and ^{173}Hg isotopes were also measured. Ground-state proton emission was identified for the new thallium isotope ^{176}Tl. As a side product of the measurement the decay of the proton-emitting ^{177}Tl nucleus was detected. In addition, the decay properties of neutron deficient ^{167,168,169,170}Pt isotopes were remeasured.

A WKB barrier transmission approximation was used to calculate the proton emission probabilities. The experimental spectroscopic factors were compared to values predicted by a low-seniority shell-model calculation assuming a near degeneracy of the $s_{1/2}$, $d_{3/2}$, and $h_{11/2}$ proton orbitals. As a result, the proton orbitals of the parent nuclei involved in the proton emission were deduced. A change in the ground-state proton configurations in odd-odd nuclei between ^{170}Au and ^{176}Tl is suggested. The results illustrate the sensitivity of the proton emission and the variety of spectroscopic information that can be obtained via proton emitting nuclei beyond the proton drip line.

ACKNOWLEDGMENTS

The authors would like to thank Geirr Sletten and Jette Sørensen at NBI, Denmark for preparing the target and Sean Freeman at Manchester University, UK for providing the ^{96}Ru material. We also thank Robert Page at Liverpool University, UK for the use of the ^{78}Kr gas. This work was supported by the Academy of Finland under the Finnish Centre of Excellence Programme 2002-2005 (Project No. 44875, Nuclear and Condensed Matter Physics Programme at JYFL) and by the EU under the RTD project EXOTAG (Contract No. HPRI-CT-1999-50017). A.K. would like to acknowledge financial support provided by the European Community program “Improving Human Research Potential and the Socio-economic Knowledge Base” Contract No. HPMF-CT-2000-01115.

[1] P. Möller, J. R. Nix, W. D. Myers, and W. J. Swiatecki, At. Data Nucl. Data Tables **59**, 185 (1995).
[2] C. N. Davids, P. J. Woods, J. C. Batchelder, C. R. Bingham, C. J. Blumenthal, L. T. Brown, B. C. Busse, L. F. Conticchio, T. Davinson, S. J. Freeman, D. J. Henderson, R. J. Irvine, R. D. Page, H. T. Penttilä, D. Seweryniak, K. S. Toth, W. B. Walters, and B. E. Zimmerman, Phys. Rev. C **55**, 2255 (1997).
[3] Sven Åberg, Paul B. Semmes, and Witold Nazarewicz, Phys. Rev. C **56**, 1762 (1997); **58**, 3011 (1998).
[4] E. Maglione and L. S. Ferreira, Eur. Phys. J. A **15**, 89 (2002).
[5] C. N. Davids, P. J. Woods, D. Seweryniak, A. A. Sonzogni, J. C. Batchelder, C. R. Bingham, T. Davinson, D. J. Henderson, R. J. Irvine, G. L. Poli, J. Uusitalo, and W. B. Walters, Phys. Rev. Lett. **80**, 1849 (1998).
[6] Cary N. Davids and Henning Esbensen, Phys. Rev. C **61**, 054302 (2000).
[7] S. Hofmann, *Particle Emission From Nuclei*, edited by D. N. Poenaru and M. Ivascu (CRC Press, Boca Raton, FL, 1989), Vol. 2, Chap. 2.
[8] R. J. Irvine, C. N. Davids, P. J. Woods, D. J. Blumenthal, L. T. Brown, L. F. Conticchio, T. Davinson, D. J. Henderson, J. A. Mackenzie, H. T. Penttilä, D. Seweryniak, and W. B. Walters, Phys. Rev. C **55**, R1621 (1997).
[9] G. L. Poli, C. N. Davids, P. J. Woods, D. Seweryniak, J. C. Batchelder, L. T. Brown, C. R. Bingham, M. P. Carpenter, L. F. Conticchio, T. Davinson, J. DeBoer, S. Hamada, D. J. Henderson, R. J. Irvine, R. V. F. Janssens, H. J. Maier, L. Müller, F. Soramel, K. S. Toth, W. B. Walters, and J. Wauters, Phys. Rev. C **59**, R2979 (1999).
[10] R. D. Page, P. J. Woods, R. A. Cunnungham, T. Davinson, N. J. Davis, S. Hofmann, A. N. James, K. Livingston, P. J. Sellin, and C. Shotter, Phys. Rev. Lett. **68**, 1287 (1992).
[11] K. Livingston, P. J. Woods, T. Davinson, N. J. Davis, S. Hofmann, A. N. James, R. D. Page, P. J. Sellin, and A. C. Shotter, Phys. Rev. C **48**, R2151 (1993).
[12] P. J. Woods and C. N. Davids, Annu. Rev. Nucl. Part. Sci. **47**, 541 (1997).
[13] M. H. Brennan and A. M. Bernstein, Phys. Rev. **120**, 927 (1960).
[14] V. Paar, Nucl. Phys. **A331**, 16 (1979).
[15] J. F. Ziegler, J. P. Biersack, and U. Littmark, *The Stopping and Range of Ions in Solids* (Pergamon, New York, 1999).
[16] M. Leino, J. Äystö, T. Enqvist, P. Heikkinen, A. Jokinen, M. Nurmia, A. Ostrowski, W. H. Trzaska, J. Uusitalo, P. Armbuster, and V. Ninov, Nucl. Instrum. Methods Phys. Res. B **99**, 653 (1995).
[17] H. Kettunen, P. T. Greenlees, K. Helariutta, P. Jones, R. Julin, S. Juutinen, P. Kuusiniemi, M. Leino, M. Muikku, P. Nieminen, and J. Uusitalo, Acta Phys. Pol. B **32**, 989 (2001).
[18] H. Kettunen, S. Eekhaudt, T. Enqvist, T. Grahn, P. T. Greenlees, P. Jones, R. Julin, S. Juutinen, A. Keenan, P. Kuusiniemi, M. Leino, A.-P. Leppänen, P. Nieminen, J. Pakarinen, C. Scholey, and J. Uusitalo, in Proton-Emitting Nuclei, edited by Enrico Maglione and Francesca Soramel, AIP Conf. Proc. No. 681 (AIP, Melville, NY, 2003), p. 26.
[19] K.-H. Schmidt, C.-C. Sahm, K. Pielenz, and H.-G. Clerc, Z. Phys. A **316**, 19 (1984).
[20] K.-H. Schmidt, Eur. Phys. J. A **8**, 141 (2000).
[21] T. Bäck, B. Cederwall, K. Lagergren, R. Wyss, A. Johnson, D. Karlgren, P. Greenlees, D. Jenkins, P. Jones, D. T. Joss, R. Julin, A. Keenan, H. Kettunen, P. Kuusiniemi, M. Leino, A.-P. Leppänen, M. Muikku, P. Nieminen, J. Pakarinen, P. Rahkila, and J. Uusitalo, Eur. Phys. J. A **16**, 489 (2003).
[22] C. R. Bingham, K. S. Toth, J. C. Batchelder, D. J. Blumenthal, L. T. Brown, B. C. Busse, L. F. Conticchio, C. N. Davids, T. Davinson, D. J. Henderson, R. J. Irvine, D. Seweryniak, W. B. Walters, P. J. Woods, and B. E. Zimmerman, Phys. Rev. C **54**, R20 (1996).
[23] R. D. Page, P. J. Woods, R. A. Cunningham, T. Davinson, N. J. Davis, A. N. James, K. Livingston, P. J. Sellin, and A. C. Shotter, Phys. Rev. C **53**, 660 (1996).
[24] F. D. Becchetti and G. W. Greenlees, Phys. Rev. **182**, 1190 (1969).
[25] J. O. Rasmussen, Phys. Rev. **113**, 1593 (1959).
[26] H. Mahmud, C. N. Davids, P. J. Woods, T. Davinson, A. Heinz, J. J. Ressler, K. Schmidt, D. Seweryniak, J. Shergur, A. A. Sonzogni, and W. B. Walters, Eur. Phys. J. A **15**, 185 (2002).
[27] Cary N. Davids and Henning Esbensen, Phys. Rev. C **64**, 034317 (2001).
[28] K. Hagino, Phys. Rev. C **64**, 041304(R) (2001).
[29] D. Seweryniak, J. Uusitalo, M. P. Carpenter, D. Nisius, C. N. Davids, C. R. Bingham, L. T. Brown, L. Conticchio, C. J. Henderson, R. V. F. Janssens, W. B. Walters, J. Wauters, and P. J. Woods, Phys. Rev. C **60**, 031304 (1999).
[30] A. Rytz, At. Data Nucl. Data Tables **47**, 205 (1991).
[31] J. Uusitalo, M. Leino, R. G. Allatt, T. Enqvist, K. Eskola, P. T. Greenlees, S. Hurskanen, A. Keenan, H. Kettunen, P. Kuusiniemi, R. D. Page, and W. H. Trzaska, Z. Phys. A **358**, 375 (1997).
[32] G. Audi, O. Bersillon, J. Blachot, and A. H. Wapstra, Nucl. Phys. **A624**, 1 (1997).
[33] A. Melerangi, D. Appelbe, R. D. Page, H. J. Boardman, P. T. Greenlees, P. Jones, D. T. Joss, R. Julin, S. Juutinen, H. Kettunen, P. Kuusiniemi, M. Leino, M. H. Muikku, P. Nieminen, J. Pakarinen, P. Rahkila, and J. Simpson, Phys. Rev. C **68**, 041301(R) (2003).
[34] P. J. Sellin, P. J. Woods, T. Davinson, N. J. Davis, A. N. James, K. Livingston, R. D. Page, and A. C. Shotter, Z. Phys. A **346**, 323 (1993).
[35] K.-N. Huang and H. Mark, At. Data Nucl. Data Tables **18**, 243 (1976).